

Variational study of the Holstein polaron

O. S. Barišić

Institute of Physics, Bijenička c. 46, HR-10000 Zagreb, Croatia

(December 2, 2024)

Abstract

The paper deals with the ground and the first excited state of the polaron in the one dimensional Holstein model. Various variational methods are used to investigate both the weak coupling and strong coupling cases, as well as the crossover regime between them. Two of the methods, which are presented here for the first time, introduce new elements to the understanding of the nature of the polaron. Reliable numerical evidence is found that, in the strong coupling regime, the ground and the first excited state of the self-trapped polaron are well described within the adiabatic limit. The lattice vibration modes associated with the self-trapped polarons are analyzed in detail, and the frequency softening of the vibration mode at the central site of the small polaron is estimated. It is shown that the first excited state of the system in the strong coupling regime corresponds to an excitation of the soft phonon mode, within the polaron. In the crossover regime, the ground and the first excited state of the system can be approximated as a mixture of the self-trapped and the delocalized polaron state. In this way, the connection between the behavior of the ground and the first excited state is qualitatively explained.

I. INTRODUCTION

Ever since Landau¹ suggested that the electron can be trapped by the deformable lattice, strongly coupled electron-phonon systems have been the subject of intensive examination. Besides the investigations of those systems in which the lattice is coupled to the whole electronic band, there has been significant interest in the physics of a single polaron, in which the electron and the associated lattice deformation form a quasi-particle, spatially and spectrally decoupled from the rest of the system. Lattice degrees of freedom make even a single polaron problem a many-body one. The analytical and numerical examinations of most electron-phonon models are thus difficult. For this reason, even the simple Holstein model² (suggested in 1959) is still being investigated in recent works. Various methods have been proposed in order to calculate the polaron ground state of the Holstein model. Almost exact results (except in the adiabatic limit) have been obtained with the quantum Monte Carlo calculations,^{3,4} the Global-Local method,⁵ the density matrix renormalization group method,⁶ and some exact diagonalization methods.^{22–24}

It is well known that the ground state of the Holstein system changes from the delocalized polaron state, where the electron is nearly free, to the small and self-trapped polaron state as the electron-phonon coupling, g , increases. These two opposite limits are usually identified as the weak and strong coupling regimes, respectively. Although it has been proved that the change of the polaron with g is smooth,⁷ the physics of the rapid crossover between the two limits in the small interval of g 's (the crossover regime) is not completely clear. Moreover, it has been claimed in Ref. 24 that the phonon excitation associated with the first excited state of the system is uncorrelated to the electron in the weak coupling regime, while it is confined to the electron in the strong coupling regime. The transition occurs in the crossover regime where, in addition, the energy difference between the ground and excited states becomes small.

The exact ground state is also an eigenstate of the system momentum.⁸ Therefore, the polaron ground state is delocalized for all parameters. However, in the strong coupling regime the effective transfer integral, t_{pol} , of the polaron hopping to neighboring sites becomes negligible, leading to self-trapped polaron states. According to Ref. 9, the dynamics of the small self-trapped polaron can be separated into two time scales. On the short time scale, the lattice deformation is centered at some lattice site, while the electron can virtually hop among the neighboring lattice sites not occupied by the deformation. Only after a certain number of such events (of the order t_{pol}/t , where t is the electron hopping integral) the polaron as a whole tunnels to a new central site. Thus, the localized polaron states may lead to a very accurate estimation of the polaron ground state energy in the strong coupling regime.

The main goal of this paper is to determine the elements important for the qualitative description of the polarons in the whole range of electron-phonon couplings. Some of them, although already known, are found to be better understood when supplemented with additional details. The excited polaron states are treated by a new method which uses a variational approach in order to define and solve a generalized eigenvalue problem. Even if this method does not converge systematically, it does provide new results concerning the nature of the polaron. For the self-trapped polarons, an exact diagonalization method to calculate the localized polaron states, rather than the translationally invariant ones, is used.

By comparison to the results of other methods, it is shown that this approach introduces only minor errors in the ground state energy of the self-trapped polaron. In addition, unlike other approaches, this method is able to compute accurately self-trapped polaron states in the regime of very large t , i.e. in the adiabatic limit. The results relevant to this limit are of physical interest due to the fact that in many materials, the effective mass of the charge carrier is much smaller than the mass associated with the phonon frequency. Finally, the self-trapped polaron states are analyzed by calculating the local electron density, the mean lattice deformation, and characteristics of the on-site zero point motions.

II. GENERAL

The Holstein Hamiltonian reads

$$\begin{aligned} \hat{H} = & -t \sum_{n,s} c_{n,s}^\dagger (c_{n+1,s} + c_{n-1,s}) + \hbar\omega \sum_n b_n^\dagger b_n \\ & - g \sum_{n,s} c_{n,s}^\dagger c_{n,s} (b_n^\dagger + b_n) . \end{aligned} \quad (1)$$

It describes the tight-binding electrons in the nearest-neighbor approximation, coupled to one branch of dispersionless optical phonons. $c_{n,s}^\dagger$ is the creation operator for the electron of spin s at lattice site n , and b_n^\dagger is creation operator for the phonon. t is the transfer (hopping) integral of the electron. $\hbar\omega$ and g are the phonon and the electron-phonon coupling energies, respectively. The Holstein Hamiltonian depends only on two ratios of relevant energy parameters: $g/\hbar\omega$ and $t/\hbar\omega$, i.e. the results will use $\hbar\omega$ as the energy unit. It is often convenient to express the lattice vibrations in terms of the nuclei space and momentum coordinates,

$$\hat{x}_n = x_0 (b_n^\dagger + b_n) , \quad \hat{p}_n = ip_0 (b_n^\dagger - b_n) , \quad (2)$$

where $x_0 = \sqrt{\hbar/2M\omega}$ and $p_0 = \sqrt{M\hbar\omega/2}$ are space and momentum uncertainties of the harmonic oscillator ground state. M is the mass of a nucleus and κ denotes the spring constant, $\omega^2 = \kappa/M$. By noting that the electron-lattice displacement coupling constant α , in $g = \alpha x_0$, is independent of M , an alternative set of Holstein Hamiltonian parameters can be introduced,

$$t = \hbar^2/2m_{el}a^2 , \quad M = \frac{\kappa}{\omega^2} , \quad \varepsilon_p = \frac{\alpha^2}{2\kappa} = \frac{g^2}{\hbar\omega} ,$$

which is convenient for the discussion of the adiabatic regime $M \gg m_{el}$. Here, m_{el} is the electron effective mass and a is the lattice constant. It is worth noting that t and ε_p (the binding energy of the polaron for $t = 0$) are independent of M and thus they are the only parameters relevant in the adiabatic limit.

By using standard conventions for $c_{k,s}^\dagger$ and b_q^\dagger ,

$$c_{k,s}^\dagger = 1/\sqrt{N} \sum_n e^{-ikna} c_{n,s}^\dagger , \quad b_q^\dagger = 1/\sqrt{N} \sum_n e^{-iqna} b_n^\dagger ,$$

Eq. (1) can be rewritten in momentum space and divided in two mutually commuting parts, $\hat{H} = \hat{H}_{k,q \neq 0} + \hat{H}_{q=0}$,

$$\begin{aligned}
\hat{H}_{k,q \neq 0} &= -2t \sum_{k,s} \cos(ka) \hat{n}_{k,s} + \hbar\omega \sum_{q \neq 0} \hat{n}_q \\
&\quad - g/\sqrt{N} \sum_{k,s,q \neq 0} c_{k+q,s}^\dagger c_{k,s} (b_q + b_{-q}^\dagger) , \\
\hat{H}_{q=0} &= \hbar\omega \hat{n}_{q=0} - gN_{el}/\sqrt{N} (b_{q=0} + b_{q=0}^\dagger) ,
\end{aligned}$$

where $\hat{n}_{k,s} = c_{k,s}^\dagger c_{k,s}$, $\hat{n}_q = b_q^\dagger b_q$, and $N_{el} \equiv \sum_{k,s} \hat{n}_{k,s}$. The part which involves only the $q = 0$ phonon mode, $\hat{H}_{q=0}$, can easily be transformed into the diagonal form, by using the unitary operator $\hat{S}_q(\xi)$,

$$\begin{aligned}
\hat{S}_q(\xi) &= \exp(\xi b_q^\dagger - \xi^* b_q) \\
\hat{S}_{q=0}^{-1}(\xi) \hat{H}_{q=0} \hat{S}_{q=0}(\xi) &= \hbar\omega \hat{n}_{q=0} - (N_{el}g)^2/N\hbar\omega ,
\end{aligned}$$

where $\xi = N_{el}g/\sqrt{N}\hbar\omega$.

Any eigenstate of $\hat{H}_{q=0}$, $\hat{S}_{q=0}(\xi)|n_{q=0}\rangle$, has the same mean total lattice deformation, $\bar{x}_{tot} = \sum_n \bar{x}_n$,

$$\begin{aligned}
\bar{x}_{tot} &= x_0\sqrt{N}\langle n_{q=0} | \hat{S}_{q=0}^{-1}(\xi) (b_{q=0}^\dagger + b_{q=0}) \hat{S}_{q=0}(\xi) | n_{q=0} \rangle \\
&= x_0\sqrt{N}(\xi^* + \xi) = 2x_0N_{el}g/\hbar\omega ,
\end{aligned} \tag{3}$$

which is independent of t . Since the $q = 0$ part of the Hamiltonian is unaffected by $\hat{H}_{k,q \neq 0}$, it can be concluded that this is also valid for all eigenstates of the total Holstein Hamiltonian. The phonon part of these eigenstates can be represented in the form of a direct product of two groups of states, the first one includes $q \neq 0$ phonon modes, while the second includes only the $q = 0$ phonon mode. This is useful because one can always check approximate computations by calculating \bar{x}_{tot} , or include this property in the computation itself. This specific property of the $q = 0$ mode is not restricted to the particular dimension of the system, nor to the number of electrons. Moreover, it can also be found in some other models where the electron-phonon coupling is the lattice deformation linearly coupled to the local electron density. A hint in this direction was reported first in Ref. 10.

The total momentum of the system, \hat{K} , is the sum of the electron and phonon momenta,

$$\hat{K} = \sum_k k \hat{n}_k + \sum_q q \hat{n}_q ,$$

and it commutes with the Hamiltonian. In the present treatment, only the low energy polaron states (the low lying states of the system for which the electron and lattice part of the wave function are spatially bound), are explicitly calculated. In this case, the total momentum K of the system is also the polaron momentum.

III. METHODS

The eigenstate computations reported here are based on the variational approach. Still, from the mathematical and physical point of view, there are quite a lot of differences among them. Therefore, each method will be described separately in this section. Those methods

with a small number of variational parameters help us to understand the basic properties of the polarons in different regimes of the Holstein model. On the other hand, methods with a very large number of variational parameters are necessary to obtain nearly exact results for the polaron states.

Let us start with a simple localized polaron wave function formed as a product of the electron and the lattice part, centered at the lattice site j ,

$$|\varphi_j\rangle = \left(\sum_n \eta_n c_{j+n}^\dagger\right) \left(\prod_m S_{j+m}(\xi_m)\right) |0\rangle. \quad (4)$$

Here, η_n is the normalized electron function at site $j+n$, $\sum_n \eta_n^* \eta_n = 1$, while $S_{j+m}(\xi_m) = \exp(\xi_m b_{j+m}^\dagger - \xi_m^* b_{j+m})$ denotes the coherent state operator acting on site $j+m$, with a complex amplitude, $\xi_m = \Re(\xi_m) + i\Im(\xi_m)$. It is easy to see that operator $S_{j+m}(\xi_m)$ shifts the space and momentum coordinates of lattice vibration at a site $j+m$ by $2\Re(\xi_m)x_0$ and $2\Im(\xi_m)p_0$, respectively,

$$S_{j+m}(\xi_m) = e^{[i2\Im(\xi_m)p_0\hat{x}_{j+m}/\hbar]} e^{[-i2\Re(\xi_m)x_0\hat{p}_{j+m}/\hbar]} \times e^{[i\Re(\xi_m)\Im(\xi_m)]}.$$

The variational energy of the state (4), \overline{E}_φ , is independent of j , and is given by

$$\begin{aligned} \overline{E}_\varphi = & -t \sum_n \eta_n^* (\eta_{n-1} + \eta_{n+1}) + \hbar\omega \sum_n |\xi_n|^2 \\ & - g \sum_n |\eta_n|^2 (\xi_n + \xi_n^*). \end{aligned} \quad (5)$$

The minimization of the energy with respect to ξ_n establishes a simple relationship between the lattice mean deformation and electron density $\varrho_n = |\eta_n|^2$,

$$\xi_n = g/\hbar\omega \varrho_n \quad \Rightarrow \quad \bar{x}_n = \alpha/\kappa \varrho_n, \quad (6)$$

so that only the equation for η_n has to be solved. The well known approximate solution to this problem is the large Holstein polaron² valid in the long wave limit,

$$\eta_n = \frac{1}{\sqrt{2d_{pol}}} \cosh^{-1}(n/d_{pol}) \quad , \quad d_{pol} = \frac{2t \hbar\omega}{g^2} = \frac{2t}{\varepsilon_p}. \quad (7)$$

The numerical scheme suggested in Ref. 11, and denoted here as L (L for localized), has no such restrictions and is used here in order to obtain the exact minimum of Eq. (5). The energy, henceforth referred to as E_L , depends only on two relevant Hamiltonian parameters, t and $g^2/\hbar\omega = \varepsilon_p$, and therefore E_L and \bar{x}_m^L are both independent of M . For this reason Eq. (6) is sometimes referred to as the adiabatic locking of electron and lattice coordinates.

Next, we shall study a translationally invariant solution composed of a linear superposition of the localized states,

$$|\Psi_K\rangle = \frac{1}{\sqrt{N_\Psi}} \sum_j e^{iKja} |\varphi_j\rangle. \quad (8)$$

$|\Psi_K\rangle$ describes the polaron state with the momentum K . A similar type of function was first proposed by Toyozawa.¹² In the present work, $\sum_m \xi_m = g/\hbar\omega$ is used so that the mean total deformation of function (8) satisfies Eq. (3),

$$\bar{x}_{tot} = x_0 \sum_m \langle \Psi_K | (b_m^\dagger + b_m) | \Psi_K \rangle = 2x_0 g / \hbar\omega .$$

The expectation value of the polaron energy, \bar{E}_Ψ , may be written in terms of $|\varphi_j\rangle$,

$$\bar{E}_\Psi = \frac{\sum_\Delta e^{iK\Delta a} \langle \varphi_j | \hat{H} | \varphi_{j+\Delta} \rangle}{\sum_\Delta e^{iK\Delta a} \langle \varphi_j | \varphi_{j+\Delta} \rangle} = \frac{\sum_\Delta e^{iK\Delta a} E_\Delta}{\sum_\Delta e^{iK\Delta a} S_\Delta} . \quad (9)$$

E_Δ and S_Δ are given in the Appendix. A simple method for calculating the minimum of the energy \bar{E}_Ψ has not yet been proposed, but accurate results have been obtained in Ref. 13 by using the Toyozawa method, which includes a very large number of variational parameters. Some additional approximations may be found in Refs. 10,14–18. The approximation used here simplifies the general expression in Eq. (8) by introducing the exponential form for functions η_n and ξ_m ,¹⁶

$$\eta_n = CG^{|n|} , \quad \xi_m = AB^{|m|} e^{iKma} , \quad 0 < G, B < 1 . \quad (10)$$

Eq. (10) defines a polaron function, $|\Psi_K(G, B)\rangle$, which is completely determined by two parameters, G and B .

In what follows, two different approaches are presented. The first, denoted by the index T (T for translational), treats G and B as the variational parameters for which the energy minimum, E_T , has to be found, and its corresponding polaron function is $|\Psi_K^T\rangle$. The T method gives good results in the weak and the strong coupling regime. Namely, in both of these limits, the $|\Psi_K^T\rangle$ function becomes similar to the polaron function obtained by the appropriate perturbative calculations.

In the second approach, presented here for the first time, the variational method is used to define a generalized eigenvalue problem as follows. The polaron wave function, denoted by index CT (CT for combination of translational functions), is rewritten as a linear combination of $|\Psi_K(G_n, B_n)\rangle$ functions,

$$|\Phi_K^{CT}\rangle = \sum_{n=1}^p a_n |\Psi_K(G_n, B_n)\rangle . \quad (11)$$

It is understood here that the functions $|\Psi(G_n, B_n)\rangle$ form a set of p generally nonorthogonal functions, defined by p different pairs (G_n, B_n) of parameters. Again, the coefficients a_n should be determined from the requirement that the expectation value of the energy,

$$\bar{E}_{CT} = \frac{\langle \Phi_K^{CT} | \hat{H} | \Phi_K^{CT} \rangle}{\langle \Phi_K^{CT} | \Phi_K^{CT} \rangle} ,$$

is minimal,

$$\partial \bar{E}_{CT} / \partial a_n^* = 0 , \quad 1 \leq n \leq p ,$$

or,

$$\begin{aligned}
& \sum_{n'} \langle \Psi_K(G_n, B_n) | \hat{H} | \Psi_K(G_{n'}, B_{n'}) \rangle a_{n'} \\
& = E_{CT} \sum_{n'} \langle \Psi_K(G_n, B_n) | \Psi_K(G_{n'}, B_{n'}) \rangle a_{n'} .
\end{aligned}$$

The solution of this generalized eigenvalue problem is a set of p orthogonal polaron functions, $|\Phi_{K,m}^{CT}\rangle$, with corresponding energies $E_{CT}^{(m)}$. The ground state energy is $E_{CT}^{(0)}$. One may always include the function $|\Psi_K^T\rangle$ in the sum (11) in order to ensure that the energy $E_{CT}^{(0)}$ is the same or better than E_T , the energy computed by the T method. Moreover, by paying some further attention to the starting set of functions, $|\Psi_K(G_n, B_n)\rangle$, in Eq. (11), one is able to investigate the first excited state $|\Phi_{K,m=1}^{CT}\rangle$ of the system, when this state corresponds to an excited polaron. The best results for the CT method are obtained when the number p of $|\Psi_K(G_n, B_n)\rangle$ functions in Eq. (8) changes with the Hamiltonian parameters. The special case, where the CT method is used with constant $p = 2$, is denoted by the index CT^2 .

Finally, this paper presents the results of two numerical exact diagonalization methods.^{19–24} In order to compute the low energy polaron states, one approximates the infinite dimensional Hamiltonian matrix with a finite one. The lowest eigenvalue and eigenvector of such a reduced Hilbert space correspond to the polaron energy and wave function, respectively. For a large sparse matrix, the energy and the wave function can be calculated very accurately, by using an appropriate numerical scheme, in the present case the Lanczos algorithm.

The two exact diagonalization methods used here differ in the choice of the basis of the Hilbert space. In the first method,²⁴ denoted by eT (e stands for exact diagonalization and T for translational), the general orthonormal state is given by

$$\begin{aligned}
& |n_0, n_{-1}, n_1, \dots, n_m, \dots\rangle_K^{eT} = \\
& \frac{1}{\sqrt{N}} \sum_j e^{iKja} c_j^\dagger |n_0, n_{-1}, n_1, \dots, n_m, \dots\rangle_j ,
\end{aligned} \tag{12}$$

which describes an eigenstate of the system with momentum K . n_m is the number of phonons at the m -th lattice site away from the electron. For example, at the electron site, and at the nearest neighbor lattice sites left and right from the electron, there are n_0 , n_{-1} , and n_1 phonons, respectively. The Hamiltonian (1) does not mix states (12) with different momenta. Therefore, the polaron function obtained by the eT method has the same K momentum as the basis states. The current implementation of the eT method is highly accurate, and from a practical point of view may be treated as exact.²⁴ For this reason, the eT results can be used to determine the numerical errors present in the other methods.

In the second exact diagonalization method, denoted by eL (e stands for exact diagonalization and L for localized), the general orthonormal state of the chosen basis is more complicated,

$$\begin{aligned}
& |i, n_0, n_{-1}, n_1, \dots, n_m, \dots; \xi_m\rangle_j^{eL} = \\
& c_{j+i}^\dagger \left[\prod_m S_{j+m}(\xi_m) \right] |n_0, n_{-1}, n_1, \dots, n_m, \dots\rangle_j .
\end{aligned} \tag{13}$$

Here the i and m indices are given with respect to the center of polaron, which is placed at the site j . Thus c_{j+i}^\dagger creates an electron at the i -th site from the polaron center at j , n_m is

the number of extra phonons at the m -th site away of the polaron center, when the lattice is already distorted by the coherent state operators $S_{j+m}(\xi_m)$, i.e. $\bar{x}_{j+m} = 2x_0\xi_m$. The eL method is used to calculate the localized polaron states. For a given set of Hamiltonian parameters, ξ_m are calculated by the L method, by minimizing the energy (5), $\xi_m = \xi_m^L$. The additional phonon excitations, counted by n_m , are necessary to obtain the actual lattice equilibrium positions of the localized polaron state and the zero point motion of the renormalized lattice vibrations.

The minimal number of states of the reduced basis necessary to obtain accurate results depends on the Hamiltonian parameters. For the eT method (12), this number increases very rapidly for $\hbar\omega \ll g, t$, which prevents the use of this method for both large g and t .

Eq. (13) describes a localized state. Therefore, the eL method is accurate only in the self-trapped polaron regime where the effects of polaron delocalization are negligible. The lattice deformation of the self-trapped polaron is approximately taken care of by the product of the coherent states operators, $\prod_m S_{j+m}(\xi_m)$, which keeps the necessary number of states (13) in the eL method calculation, relatively small. Thus, nearly exact results can be obtained even for very large g and t , in the self-trapped polaron regime. In order to reduce the basis of the Hilbert space, the maximal allowed distance of the electron and phonons from the polaron center has been limited by the choice $|i|, |m| \leq D^{max}$. The distance D^{max} has been determined from the condition that $\xi_m/\xi_0 < 10^{-4}$ if $m \geq D^{max}$. The maximal total number of phonons has been kept limited, such that $\sum_m n_m \leq 4$. However, both criteria depend on Hamiltonian parameters. As the sum $\sum_m n_m$ does not include the phonons associated with the coherent state operators, $S_{j+m}(\xi_m)$, the small value of $\sum_m n_m$ is not a restriction on the amplitude of the lattice deformation.

For the purpose of clarity, it seems appropriate to briefly review the notation of all five presented methods, the L , T , CT , eT and eL methods. All methods based on the localized polaron function are denoted by the letter L (L and eL methods), whereas all methods based on the translational function are denoted by the letter T (T , CT and eT methods). The letter e denotes an exact diagonalization method (eT and eL methods), whilst a single letter notation (L and T) suggest a simple method.

IV. PROPERTIES OF THE POLARON MOTION AND THE POLARON SIZE

The different regimes of the Holstein polaron are frequently determined from the polaron dynamical properties. In the present paper the weak coupling regime is viewed as the regime of delocalized polaron states with momentum K . The mobility of these states is only slightly smaller than the mobility of the free electron. The strong coupling regime is viewed as the regime of self-trapped polaron states, whose mobility is negligible. The regime in which polaron states change from delocalized to self-trapped ones, as the electron-phonon coupling g increases, corresponds to the crossover regime. Although this interpretation of the parameter regimes is not unique, it does appear to emerge naturally from the properties of the polaron motion.

The location of the crossover regime has been estimated in Ref. 25 from the analysis of the effective polaron mass. The authors have selected the point of most rapid increase in effective mass as the crossover point. They have concluded, on the basis of the Global-Local

method for $0.1 \hbar\omega < t < 10 \hbar\omega$, that the crossover value of the electron-phonon coupling constant is given by the "self-trapping line" in the $g - t$ parameter space,

$$g_{ST} = \hbar\omega + \sqrt{t \hbar\omega} . \quad (14)$$

Relation (14) can be qualitatively understood in terms of the two opposite limits of t for which the *small* polaron regime can be invoked. For small t , when $g_{ST}/\hbar\omega \approx 1$, the mean phonon number associated with the lattice deformation is approximately equal to one, $\overline{N}_{tot} \approx 1$. The case $\overline{N}_{tot} > 1$ corresponds to the self-trapping regime (large effective polaron mass), while $\overline{N}_{tot} < 1$ makes the free electron state the dominant part in the total polaron wave function. Such a polaron cannot be self-trapped, even in the $t \rightarrow 0$ limit. For large t in Eq. (14), $g_{ST}^2/\hbar\omega \approx t$, and the electron-lattice interaction energy for small polaron is comparable to the energy gain of the electron hopping to the neighboring site.

The polaron dynamical properties are characterized by three energies, t and t_{pol} , the energies of electron and polaron hopping to neighboring sites, respectively, and $\hbar\omega$, which is the vibrational energy of the lattice deformation. The relationship between t_{pol} and the Hamiltonian parameters, t and $\hbar\omega$, is determined by g . For example, in the weak coupling regime, the influence of the lattice deformation on polaron dynamics is very small, which makes the energies of electron and polaron motion similar, $t_{pol} \lesssim t$. In the strong coupling regime, the lattice deformation reduces t_{pol} to such small values that it can be neglected, $t_{pol} \ll t, \hbar\omega$.

The nature of polaron self-trapping can be discussed by analyzing the properties of the two polaron wave functions given by (4) and (8). When the localized polaron functions $|\varphi_j\rangle$ at different lattice sites are not orthogonal, $\langle\varphi_j|\varphi_{j'}\rangle \neq \delta_{j,j'}$, the local properties and delocalization effects of $|\Psi_K\rangle$ are a complex mixture. However, in both the weak and strong coupling regimes, the translational polaron function can be approximately written in terms of orthogonal localized polaron functions. In the weak coupling regime, the orthogonality follows from the electron part of the wave function,

$$\langle\varphi_j|\varphi_{j'}\rangle \sim \sum_n \eta_{j+n}^* \eta_{j'+n} \approx \delta_{j,j'} ,$$

while in the strong coupling regime, it follows from the lattice part,

$$\langle\varphi_j|\varphi_{j'}\rangle \sim Y_{j'-j} = \exp \left[-\frac{1}{2} \sum_m (\xi_{j+m}^* - \xi_{j'+m})^2 \right] \approx \delta_{j,j'} . \quad (15)$$

The condition (15) corresponds to the regime of a self-trapped polaron. Namely, the translational form of the polaron function (8) has a negligible energy contribution in the limit $Y_{\Delta \neq 0} \rightarrow 0$, and the minimal values of the variational energies (5) and (9) coincide, i.e. $E_{\Delta}, S_{\Delta} \sim Y_{\Delta}$ in Eq. (9).

The small contribution of the lattice part to the overlap of two localized neighboring polaron functions in Eq. (15) results in a small t_{pol} . In the present work, the estimation of t_{pol} is based on the evaluation of Y_1^L from Eq. (15) for two neighboring $|\varphi_j^L\rangle$ functions,

$$t_{pol} \sim t_{pol}^L = t Y_1^L = t \exp \left[-\frac{1}{2} \sum_m (\xi_m^L - \xi_{m+1}^L)^2 \right] . \quad (16)$$

By neglecting the motion of the self-trapped polaron one neglects only a contribution of order t_{pol} to the total polaron energy. It is thus appropriate to consider the strong coupling regime as the regime in which the polaron states are very well approximated by the localized states centered at some lattice sites j .

In Fig. 1 two characteristic curves t_{pol}^L are plotted in the $g - \sqrt{t}$ parameter space. The long-dashed and the solid curves correspond to $t_{pol}^L = 10^{-1} \hbar\omega$ and $t_{pol}^L = 10^{-9} \hbar\omega$, respectively, meaning that in the region between them, the increase of g reduces t_{pol} for eight orders of magnitude. The region between the curves is therefore qualitatively equivalent to the crossover regime in which t_{pol} becomes negligible. The thin dot-dashed line in Fig. 1 corresponds to g_{ST} , Eq. (14). For large t , it does overestimate the value of g at which the polaron self-trapping occurs. Nevertheless, in the region of parameters for which g_{ST} was originally proposed (smaller g and t), Eq. (14) is consistent with the polaron crossover regime presented here.

V. STRONG COUPLING LIMIT

The self-trapped polaron states are usually analyzed in the regime of parameters which corresponds to small polarons as well. However, unlike the polaron mobility, the polaron size does not necessarily become small as t_{pol} vanishes. The polaron size is appropriately defined as the quantity which measures the number of lattice sites to which the lattice deformation is spread, with respect to the electron. In this respect, the calculation of the polaron size σ is based on the behavior of the correlation function between the electron density and the lattice deformation, $C(r)$,²⁶

$$C(r) = \frac{\hbar\omega}{2g} \langle \Psi | \sum_n c_n^\dagger c_n (b_{n+r}^\dagger + b_{n+r}) | \Psi \rangle$$

$$\sigma^2 = \sum_r r^2 C(r) \quad (17)$$

If Eq. (3) is satisfied, $\sum_r C_r = 1$. For $\sigma < 1$ the lattice deformation is almost completely localized on the site occupied by the electron. The corresponding polarons may thus be identified as small polarons.

The size (17) of the translationally invariant polaron (8), $|\Psi\rangle$, may be expressed in terms of the localized polaron functions (4), $|\varphi_j\rangle$, in a form analogous to the polaron energy given in Eq. (9),

$$\sigma^2 = \frac{\sum_{\Delta} e^{iK\Delta a} \sigma_{\Delta}^2}{\sum_{\Delta} e^{iK\Delta a} S_{\Delta}}. \quad (18)$$

σ_{Δ}^2 is, like E_{Δ} and S_{Δ} , proportional to the lattice part of the overlap of two localized functions at distance Δ , $\sigma_{\Delta}^2 \sim Y_{\Delta}$ (the full expression for σ_{Δ} is given in Appendix). Therefore, in the regime of the self-trapped polarons, in which $Y_{\Delta \neq 0} \rightarrow 0$, the size of the translationally invariant polaron $|\Psi\rangle$ is simply given by the size of the localized polaron $|\varphi_j\rangle$, $\sigma = \sigma_{\Delta=0}$.

For the localized polaron states $|\varphi_j^L\rangle$ calculated by the L method, which gives good results for the mean electron density and lattice deformation of the self-trapped polarons, one obtains

$$\sigma_L^2 = \left(\frac{\hbar\omega}{g}\right)^2 \sum_{n,r} r^2 \xi_n^L \xi_{n+r}^L = \sum_{n,r} r^2 \varrho_n^L \varrho_{n+r}^L . \quad (19)$$

Due to Eq. (6) the electron and lattice coordinates in Eq. (19) are interchangeable.

The polaron function $|\varphi_j^L\rangle$ is similar to the Holstein large polaron, Eq. (7), except in the case of small polarons where the long wave approximation is inappropriate. The inset in Fig. 2 illustrates this behavior. Apart from self-trapped polarons with $\sigma^L < 2$, the self-trapped polaron size σ is a linear function of t/ε_p , as it is in Eq. (7).

In the limit of large t , Eq. (14) corresponds to the ratio $t/\varepsilon_p = 1$. Thus, in the strong coupling regime, Eq. (14) actually defines the self-trapped polaron size $\sigma^L(t/\varepsilon_p = 1) = 2.42$. A reinspection of Fig. 1 shows that for fixed $t_{pol}^L = 10^{-9} \hbar\omega$, σ increases with t , i.e. $\sigma \sim t \hbar\omega/g^2$ for the self-trapped polarons. This behavior leads to self-trapped polaron states the size of which is not necessarily small.

The eL method provides very accurate results for the ground state energy of the self-trapped polarons. For example, for electron-phonon coupling which is only greater than g_{ST} by $\hbar\omega$, i.e. $g = g_{ST} + \hbar\omega$, the maximal error of the eL method is $E_{eL} - E_{eT} < 3 \times 10^{-4} \hbar\omega$. This is shown in Fig. 2, in which t_{pol}^L , and one fourth of the polaron bandwidth computed by eT method,

$$W^{eT} = E_{eT}(K = \pi/a) - E_{eT}(K = 0) \sim 4t_{pol} ,$$

are plotted as well. All curves are of the same order of magnitude, which should be expected since all plotted quantities are closely related to the polaron hopping energy t_{pol} .

One of the advantages of the eL method is that it permits separate calculations of electron and lattice properties. For instance, for the polaron centered at the origin, the associated mean lattice deformation, \overline{x}_n , is given simply by the expectation value of \hat{x}_n . In the present paper, besides \overline{x}_n , the mean real space uncertainty of the on-site lattice vibration, $\overline{\Delta x}_n$, and the product $\overline{\Delta x}_n \overline{\Delta p}_n$, where $\overline{\Delta p}_n$ is the mean momentum uncertainty of the on-site lattice vibration, are calculated. Differences between the results of the L and the eL methods are also analyzed. It is found that they are more pronounced for small g . The lattice part of the L function describes a set of displaced harmonic oscillators, so $\Delta x_n^L = x_0$, $\Delta p_n^L = p_0$, where x_0 and p_0 are defined in Eq. (2). Fig. 3 shows the data for two sets of parameters corresponding to a small ($\sigma^L = 0.62$) and a large ($\sigma^L = 2.19$) self-trapped polaron, respectively.

We may see from the results in Fig. 3, that the mean lattice deformation differs between the L and eL methods. In the case of the eL method, it is more extended and the size of the polaron is slightly larger. Additionally, the electron density of the eL method remains approximately proportional to the mean lattice deformation (as in Eq. (6), valid for the L method), since

$$[x_n^{eL} - \frac{2g}{\hbar\omega} \varrho_n^{eL} x_0] / x_n^{eL} < 1\% .$$

Real space uncertainties of the lattice vibrations on the sites occupied by the polaron are larger in the eL case than in the L case, $\Delta x_n^{eL} > x_0$, but uncertainties of on-site momentum lattice vibrations are smaller, $\Delta p_n^{eL} < p_0$.

For small polarons the electron affects mostly the central polaron site. The product of uncertainties for this site stays close to the free lattice value, $\Delta x_{n=0}^{eL} \Delta p_{n=0}^{eL} \approx x_0 p_0$. Therefore, the phonon mode at the central site of the small polaron may be treated, in the first

approximation, as harmonic. In particular, the renormalized frequency of this mode, $\omega_{n=0}^{eL}$, can be roughly estimated from the relation

$$\Delta x_{n=0}^{eL} \approx \sqrt{\hbar/2M\omega_{n=0}^{eL}}.$$

Since $\Delta x_{n=0}^{eL} > x_0$, it follows that $\omega_{n=0}^{eL} < \omega$. Therefore, in the strong coupling regime the first excited state should correspond to the excitation of the renormalized phonon mode, rather than to the excitation of the phonon of energy $\hbar\omega$, which is uncorrelated to the polaron. One may also notice that the energy of the mean lattice deformation is larger for the eL method than the L method. This is compensated for, however, by the lower energy associated with the zero point motion of the $\omega_{n=0}^{eL}$ phonon mode, which makes the total polaron energy of the eL method lower.

In the regime of large self-trapped polarons, the renormalized normal phonon modes are expected to be spread to a number of lattice sites. Consequently, a number of different phonon modes contribute to the lattice displacement at a lattice site occupied by the polaron. Thus, the analysis of the on-site vibrations cannot give direct information on the renormalized lattice modes.

VI. WEAK COUPLING REGIME

In the weak coupling regime, the T method gives results close to the eT results. Since the form of the function T is quite simple, it will be used in this section as a basis for further discussion. In the weak coupling regime, the minimum of the variational energy, E_T , corresponds to small values of the variational parameters G and A . The standard perturbative ground state of the system with momentum K in terms of the T method polaron function may be written as follows:

$$\begin{aligned} |\Psi_K^T\rangle &= \frac{1}{\sqrt{N_\Psi}} \sum_j e^{iKja} c_j^\dagger \\ &\times (1 + A \sum_m B^{|m|} e^{iKma} b_{j+m}^\dagger) |0\rangle, \quad K < K_c, \end{aligned} \quad (20)$$

$$\begin{aligned} b_K^\dagger |\Psi_{K=0}^T\rangle &= b_K^\dagger \frac{1}{\sqrt{N_\Psi}} \sum_j c_j^\dagger \\ &\times (1 + A \sum_m B^{|m|} b_{j+m}^\dagger) |0\rangle, \quad K > K_c. \end{aligned} \quad (21)$$

For $K < K_c$ the wave function (20) has two parts. The main part corresponds to the free electron of momentum K , and the smaller part, proportional to A , corresponds to the electron dressed by one spatially correlated virtual phonon. At the threshold K_c , the energy of such a polaron state intersects with the energy of the system consisting of the zero momentum polaron and one extra phonon with momentum K_c , Eq. (21). So, for $K > K_c$ the ground state is achieved with one real phonon in the system which carries the system momentum and which is spatially uncorrelated with the polaron.^{13,27} For $K < K_c$ this state becomes the first excited state of the system. The difference between the energies of the ground state and the first excited state is the largest for $K = 0$, and it is equal to $\hbar\omega$.

The validity of the perturbative treatment requires that the weight of the second term in Eqs. (20) and (21) is small, i.e. the mean number of phonons associated with the lattice deformation has to satisfy

$$\begin{aligned}\overline{N}_{ph}^{pol} &= A^2(1+B^2)/(1-B^2) \\ &= \frac{g^2}{(\hbar\omega)^2} \frac{(1-B)(1+B^2)}{(1+B)^3} \ll 1.\end{aligned}\quad (22)$$

Here, A has been eliminated by using Eq. (3). There are two ways to satisfy condition (22). Either the electron-phonon coupling is small, $g \ll \hbar\omega$, or the lattice deformation is spread to a large number of lattice sites, $1-B \ll 1$. In the latter case, the total mean polaron deformation does not have to be small, $\overline{x}_{tot}/x_0 = 2g/\hbar\omega$, since g can be larger than $\hbar\omega$.

The translationally invariant form of the wave function for the T method, given by Eq. (8), provides an energy gain due to the polaron delocalization. At the same time, the spatial correlation between the electron and the lattice deformation has a finite length. For instance, in Eq. (8), this length is of the same order for $|\Psi_K\rangle$ and $|\varphi_j\rangle$. The perturbative calculation for B in Eq. (20) gives

$$B = \cos(Ka) + \hbar\omega/2t - \sqrt{[\cos(Ka) + \hbar\omega/2t]^2 - 1}.$$

B measures the electron-lattice correlation length, i.e. the polaron size σ . B is independent of g , which makes the correlation length finite, even in the limit $g \rightarrow 0$ for which the lattice deformation vanishes, $A \sim g/\hbar\omega$.

On the other hand, the electron-lattice deformation correlation length and the polaron delocalization range are of the same order for the localized functions. This can be easily seen from Eq. (4). In the $g \rightarrow 0$ limit they both become infinite. Thus, in the weak coupling regime one obtains a localized polaron state, $|\varphi_j^L\rangle$, of very large size, but tiny lattice deformation. This is specific to one dimensional systems where an attractive symmetric potential always has a bound electron state. Therefore, the polaron energy is less than the free electron energy $-2t$. In higher dimensions, an arbitrary attractive symmetric potential does not have a bound electron state for sufficiently small g , and the polaron energy is larger than $-2dt$, where d is the dimension of the system. This explains why, in the weak coupling regime, the localized polaron functions^{11,28,29} fail to generate a ground state energy lower than the free electron energy, for the dimension of the system greater than one. A detailed parallel perturbative analysis of polarons in one, two and three dimensions is given in Ref. 30.

VII. CROSSOVER REGIME

In the crossover regime the polaron hopping energy t_{pol} is not negligible, and the translational invariant polaron functions should be used in order to obtain the full physical picture of the nature of the polaron. In order to calculate the numerical errors of different methods accurately, the present discussion of the crossover regime is restricted to values of t smaller than $25 \hbar\omega$, for which results from the eT method are available. For such t , g_{ST} gives a satisfactory determination of the position of the crossover regime (see Fig. 1). However, the

large self-trapped polarons occur only in the case of larger t . Thus, we are simultaneously investigating the crossover regime and the transformation from large to small polarons, but this is just a consequence of the choice of parameters ($t < 25 \hbar\omega$).

In order to examine the crossover regime it is instructive to calculate the energy difference between the ground and first excited state, $E_{CT}^{(1)} - E_{CT}^{(0)}$. Let g_c denote the value of g for which this difference is minimal,

$$\partial(E_{CT}^{(1)} - E_{CT}^{(0)})/\partial g|_{g=g_c} = 0 .$$

The current results indicate that g_c is very close to the value of g_{ST} , Eq. (14), which corresponds to the crossover point. For example, for $t = 20 \hbar\omega$, $g_c = 5.55 \hbar\omega$, while $g_{ST} = 5.47 \hbar\omega$. For smaller t , g_c and g_{ST} coincide even better. The analysis of the effective mass²⁵ and variational energy of the polaron ground state,³¹ as well as the behavior of the first excitation energy, suggest that a dramatic change in the nature of the polaron ground state in the crossover regime and the first excited state are related.

This can be well understood by considering the properties of the wave function in the T method. Near g_c , this polaron wave function has two separate energy minima in the G - B parameter space which become degenerate for $g = g_c$. Let the symbol $<$ denotes the lower minimum at $g < g_c$, and the symbol $>$ the lower minimum at $g > g_c$. $|\Psi^< \rangle$ and $|\Psi^> \rangle$ are the corresponding polaron wave functions. Even if they are not mutually orthogonal, they are still physically quite different. The numerical data show that the translational invariance of $|\Psi^< \rangle$ contributes strongly to the polaron energy. On the other hand, the translational invariance of $|\Psi^> \rangle$ has almost negligible energy contributions, i.e. $|\Psi^> \rangle$ describes an almost self-trapped polaron. It is worth noting that the degenerate nature of the variational energy which has been reported for the Toyozawa method¹³ is of the same kind as the one of the T method discussed here. Namely, both T and Toyozawa method are based on the same polaron function (8).

$|\Psi^< \rangle$ and $|\Psi^> \rangle$ can be combined to form new polaron functions,

$$|\Phi^{CT^2} \rangle = a_< |\Psi^< \rangle + a_> |\Psi^> \rangle . \quad (23)$$

A similar combination of two states has been used in Ref. 32 in order to calculate the polaron ground state. $|\Phi^{CT^2} \rangle$ corresponds to Eq. (11) with $p = 2$, which means that the CT^2 method may be implied. From this treatment the improved ground state, $|\Phi_0^{CT^2} \rangle$, and the approximate first excited polaron state, $|\Phi_1^{CT^2} \rangle$, are obtained. This is illustrated in Fig. 4, where the ground state energy, E_{eT} , is subtracted from all plotted energy curves. It can be seen that in the CT^2 method, there is an anti-crossing of $|\Psi^> \rangle$ and $|\Psi^< \rangle$ states, which yields two orthogonal states, $|\Phi_0^{CT^2} \rangle$ and $|\Phi_1^{CT^2} \rangle$. For $g < g_c$ the *light* state $|\Psi^< \rangle$ is favorable in energy, and participates in the ground state more than the *heavy* state $|\Psi^> \rangle$. With the increase of g , however, this balance changes continuously in favor of $|\Psi^> \rangle$. The opposite trend is observed for the first excited state, which is heavier than the ground state for smaller g and lighter for larger g .

The CT method gives better results for the ground and first excited state when a large number of functions in Eq. (11) is used (large p). From Fig. 4, at $g = g_c$, one may estimate that $E_{CT}^{(1)} - E_{CT}^{(0)} \approx \hbar\omega/2$. Moreover, the energy $E_{CT}^{(1)}$, unlike $E_{CT^2}^{(1)}$, satisfies $E_{CT}^{(1)} < E_{eT} + \hbar\omega$ for all $g > g_c$.

VIII. SUMMARY OF THE RESULTS

A simple empirical relation derived below gives a surprisingly good estimate of the first excitation energy $E_{CT}^{(1)}$ for $g > g_{ST}$, provided t is not too large so that $g_{ST} \approx g_c$. As was already pointed out in Sec. V, the excitation of the renormalized phonon mode explains the nature of the first excited self-trapped polaron state. In Ref. 29 perturbation theory was used to calculate the frequency of this local phonon mode, ω' , to the lowest order in $t \hbar\omega/g^2$,

$$\omega' = \omega \sqrt{1 - (t \hbar\omega/g^2)^2}. \quad (24)$$

It is worth noting that the perturbative correction to the phonon frequency in Eq. (24) is adiabatic, i.e. it is independent of mass M . ω' corresponds to a phonon mode which is unstable for $g \leq \sqrt{t \hbar\omega}$. On the other hand, the CT method suggests that the critical g for the phonon stability is $g = g_c$. Namely, this is the value of g for which the first excited state is closest to the ground state energy. If Eq. (24) is combined with the relation (14) for g_{ST} (a good approximation to g_c), a new expression can be proposed for the renormalized phonon frequency, ω'' ,

$$\omega'' = \omega \sqrt{1 - [t \hbar\omega/(g - \hbar\omega)^2]^2}, \quad g > g_{ST}, \quad (25)$$

corresponding to a phonon mode which is unstable for $g \leq g_{ST}$. Moreover, by adding the phonon excitation of frequency ω'' to the ground state energy,

$$E_{emp}^{(1)} = E_{eT} + \hbar\omega'' \quad , \quad g > g_{ST}, \quad (26)$$

a relation which is a good approximation of the CT results for the energy of first excited state is obtained, $E_{emp}^{(1)} \approx E_{CT}^{(1)}$. This approximation holds well except for the obvious exception in the near vicinity of g_{ST} where $\omega'' \rightarrow 0$. Note that the renormalization factor of ω in Eq. (25) has a non-adiabatic contribution required to fit the minimum of $E_{emp}^{(1)}$ for $g = g_{ST}$. The energy $\hbar\omega'$ of the phonon excitation obtained by perturbative calculation, the energy $\hbar\omega''$ of the excitation which correspond to Eq. (26), and the excitation energy $E_{CT}^{(1)} - E_{eT}$ computed by the CT method are compared in Fig. 5.

The lattice part of the CT function is spatially symmetric with respect to the electron. Therefore, the local renormalized phonon mode of the small polaron, Eq. (25), should be basically a symmetric oscillation of the lattice deformation around the central polaron site. If g_{ST} is approached from above, the effects of the polaron delocalization become important and this mode spreads to many lattice sites as g nears g_{ST} . One may speculate that such an extended phonon is responsible for the smaller effective mass of the excited polaron state comparing to the mass of the ground state obtained for $g > g_c$. It is likely that the excitation of the renormalized phonon increases the effective polaron hopping integral.

Fig. 6 shows the results for the ground state energy and the energy of the first excited state with total system momentum $K = 0$, as functions of g , obtained by several different methods. The ground state energy obtained by eT method is subtracted from all the other results. g_1 and g_2 are used to mark three different polaron regimes with respect to the strength of the electron-phonon coupling. In the weak coupling regime, $g < g_1 = 2.37 \hbar\omega$, the mean number of phonons of the lattice deformation is less than one. For $g > g_2 = 5.25 \hbar\omega$ we

recognize the self-trapped polaron regime which, for the choice $t = 5 \hbar\omega$, corresponds to the small polaron regime as well. Namely, for $g > g_2$ the polaron hopping energy (16) satisfies $t_{pol}^L \leq 10^{-9} \hbar\omega$ and $\sigma_L \leq 0.19$. The crossover regime is found in the interval $g_1 < g < g_2$.

It may be noted from Fig. 6 that in the weak coupling regime, the energy obtained by the L method (E_L) is close to the free electron energy $-2t$ (for $t \geq 20 \hbar\omega$, the absolute error of the L method becomes greater than $\hbar\omega$ in some intervals of g). In the strong coupling regime, for large g , E_L approaches the exact polaron energy.

The error of the T method, as may be seen from Fig. 6, is the largest in the crossover regime where the results can be improved by a better choice of η_n and ξ_m in Eq. (10). In the regime of self-trapped polaron, the translationally invariant form of the function T has no effect on the polaron energy, i.e. both the T and L methods give very similar results.

The energy of the first excited polaron state, $E_{CT}^{(1)}$, intersects the energy of the ground state plus one phonon, $E_{eT} + \hbar\omega$, for $g > g_1$. After the minimum of $E_{CT}^{(1)} - E_{CT}^{(0)}$ is reached in the crossover regime at $g = g_c$, $E_{CT}^{(1)}$ approaches $E_{eT} + \hbar\omega$ asymptotically for $g > g_2$, and this is approximately described by Eq. (26).

IX. CONCLUSIONS

The present paper discusses the ground and first excited states of the polaron for three different regimes of the electron-phonon coupling parameter g . The results can be briefly summarized as follows. In the strong coupling regime the effective transfer integral of the polaron tunneling to neighboring sites is negligible, and the self-trapped polaron states are obtained. For very large t , it has been found that the regime of the large self-trapped polarons precedes the regime of the small self-trapped polaron, which is established for very large g . The results of the eL method suggest that the adiabatic picture of the localized polaron state, in which some of the local lattice vibrations are renormalized by the presence of the electron, is valid. The numerical data show no significant deviation from the adiabatic locking relation (6) of the electron site density and the mean lattice deformation. In the small polaron case, the predominant effect of the electron is a lowering of the frequency of the vibration at the central polaron site. The excitation of this renormalized phonon mode corresponds to the first excited state of the small self-trapped polaron.

The nature of the polaron ground state in the crossover regime has been discussed in a number of papers, and its rapid change with g has been well-established numerically. The difference between the energies of the first excited state and the ground state, as a function of g , has a minimum for $g = g_c$. It is showed, by using the CT^2 method, that the anti-crossing of the self-trapped and the delocalized polaron state can link the behavior of the ground and first excited polaron state. According to the CT method, for $g > g_c$ the effective mass of the ground state is larger than the effective mass of the first excited state, while for $g < g_c$ the opposite is true. In addition, g_c , which characterizes the first excited state, and g_{ST} , obtained from ground state analysis (Eq. (14)) are almost coincidental for $t < 25 \hbar\omega$. For $g > g_c$ it is argued that the local renormalized phonon mode is spread out by the effects of the polaron delocalization. This mode softens by decreasing g . This latter effect is taken into account by the simple empirical relation (26) for the excitation energy of the polaron.

Up on further reduction of g , the total mean number of phonons bound by the polaron becomes smaller than one, and the weak coupling regime is reached. The nearly free electron

is dressed by a cloud of virtual phonons, and its mass is slightly renormalized. The first excited state of the system, with momentum $K \approx 0$, can be viewed as the ground state of the polaron plus one additional uncorrelated phonon, rather than as an excited polaron.

ACKNOWLEDGMENTS

The author would like to thank I. Batistić for fruitful collaboration during the course of this work.

APPENDIX A:

In order to calculate S_Δ , E_Δ , and σ_Δ , of Eqs. (9) and (18), one may use the following expressions,

$$\begin{aligned}
Y_\Delta &= \exp \left[-\frac{1}{2} \sum_m (\xi_m^* - \xi_{m+\Delta})^2 \right] \\
S_\Delta &= Y_\Delta \sum_n \eta_n^* \eta_{n+\Delta} \\
E_\Delta &= -t Y_\Delta \sum_n \eta_n^* (\eta_{n+\Delta+1} + \eta_{n+\Delta-1}) \\
&\quad + \hbar\omega S_\Delta \sum_m \xi_m^* \xi_{m+\Delta} \\
&\quad - g Y_\Delta \sum_n \eta_n^* \eta_{n+\Delta} (\xi_n^* + \xi_{n+\Delta}) \\
C_\Delta(r) &= \frac{\hbar\omega}{2g} Y_\Delta \sum_n \eta_n^* \eta_{n+\Delta} (\xi_{n+r}^* + \xi_{n+\Delta+r}) \\
\sigma_\Delta^2 &= \sum_r r^2 C_\Delta(r) .
\end{aligned}$$

REFERENCES

- ¹ L. D. Landau, Z. Phys. **3**, 644 (1933).
- ² T. Holstein, Ann. Phys. (N.Y.) **8**, 325 (1959).
- ³ H. De Raedt and A. Langedijk, Phys. Rev. Lett. **49**, 1522 (1982); Phys. Rev. B **27**, 6097 (1983); **30**, 1671 (1984);
- ⁴ P. E. Kornilovitch and E. R. Pike, Phys. Rev. B **55**, R8634 (1997);
- ⁵ D. W. Brown, K. Lindenberg, and Y. Zhao, J. Chem. Phys. **107**, 3179 (1997).
- ⁶ C. Zhang, E. Jeckelmann, and S. R. White, Phys. Rev. Lett. **80**, 2661 (1998); E. Jeckelmann and S. R. White, Phys. Rev. B **57**, 6376 (1998).
- ⁷ H. Löwen, Phys. Rev. B **37**, 8661 (1998).
- ⁸ P. Gosar, J. Phys. C **8**, 3584 (1975).
- ⁹ A. S. Alexandrov, Phys. Rev. B **61**, 12315 (2000).
- ¹⁰ D. Feinberg, S. Ciuchi, and F. de Pasquale, Int. J. Mod. Phys. B **4**, 1395 (1990).
- ¹¹ G. Kalosakas, S. Aubry, and G. P. Tsironis, Phys. Rev. B **58**, 3094 (1998).
- ¹² Y. Toyozawa, Prog. Theor. Phys. **26**, 29 (1961).
- ¹³ Y. Zhao, D. W. Brown and K. Lindenberg, J. Chem. Phys. **107**, 3159 (1997).
- ¹⁴ H. B. Shore and L. M. Sander, Phys. Rev. B **7**, 4573 (1973).
- ¹⁵ K. H. Hock, H. Nickisch, and H. Thomas, Helv. Phys. Acta **56**, 237 (1983).
- ¹⁶ G. Venzl and S. F. Fischer, Phys. Rev. B **32**, 6437 (1985).
- ¹⁷ A. Klamt, J. Phys. C **21**, 1953 (1988).
- ¹⁸ A. La Magma and R. Pucci, Phys. Rev. B **53**, 8449 (1996).
- ¹⁹ J. Ranninger and U. Thibblin, Phys. Rev. B **45**, 7730 (1992).
- ²⁰ F. Marsiglio, Phys. Lett. A **180**, 280 (1993); Physica C **244**, 21 (1995).
- ²¹ A. S. Alexandrov, V. V. Kabanov, and D. K. Ray, Phys. Rev. B **49**, 9915 (1994).
- ²² G. Wellein and H. Fehske, Phys. Rev. B **56**, 4513 (1997).
- ²³ G. Wellein and H. Fehske, Phys. Rev. B **58**, 6208 (1998).
- ²⁴ J. Bonča, S. A. Trugman, and I. Batistić, Phys. Rev. B **60**, 1633 (1999).
- ²⁵ A. H. Romero, D. W. Brown, and K. Lindenberg, Phys. Rev. B **59**, 13728 (1999).
- ²⁶ A. H. Romero, D. W. Brown, and K. Lindenberg, Phys. Lett. A, **266**, 414 (2000).
- ²⁷ J. M. Robin, Phys. Rev. B **58**, 14335 (1998).
- ²⁸ D. Emin and T. Holstein, Phys. Rev. Lett. **36**, 323 (1976).
- ²⁹ V. V. Kabanov and O. Yu. Mashtakov, Phys. Rev. B **47**, 6060 (1993).
- ³⁰ A. H. Romero, D. W. Brown, and K. Lindenberg, Phys. Lett. A, **254**, 287 (1999).
- ³¹ A. H. Romero, D. W. Brown, and K. Lindenberg, Phys. Rev. B **60**, 4618 (1999).
- ³² V. Cataudella, G. De Filippis, and G. Iadonisi, Phys. Rev. B **60**, 15163 (1999); **62**, 1496 (2000).

FIGURES

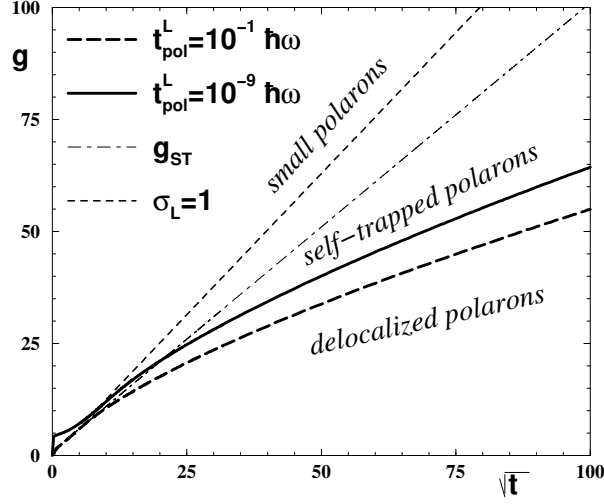


FIG. 1. The long-dashed and the solid curves divide the regimes of delocalized (below the dashed curve) and self-trapped (above the solid curve) polarons in the g - \sqrt{t} parameter space, $\hbar\omega = 1$. The region between these curves corresponds to the crossover regime in which the effective polaron hopping integral t_{pol} becomes negligible. t_{pol} is estimated by the L method by using Eq. (16). The dot-dashed line is given by Eq. (14). The regime of small self-trapped polarons ($\sigma_L < 1$) correspond to the region above the short-dashed line accordingly to Sec. V.

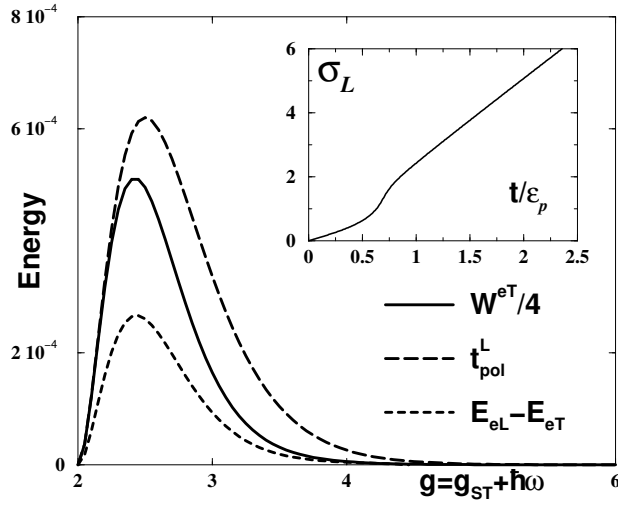


FIG. 2. The solid curve is obtained by the eT method and corresponds to one fourth of the polaron bandwidth. The long-dashed curve is the estimate of the effective polaron hopping energy obtained by Eq. (16). The short-dashed curve corresponds to the error of the polaron energy calculated by the eL method. All three curves are given as functions of the electron-phonon coupling $g = g_{ST} + \hbar\omega = \sqrt{t \hbar\omega} + 2 \hbar\omega$. The energies are given in units of $\hbar\omega$ (i.e. $\hbar\omega = 1$). In the inset, the size of the polaron σ_L which is obtained by the L method, Eq. (19), is plotted as a function of $t/\epsilon_p = t \hbar\omega/g^2$.

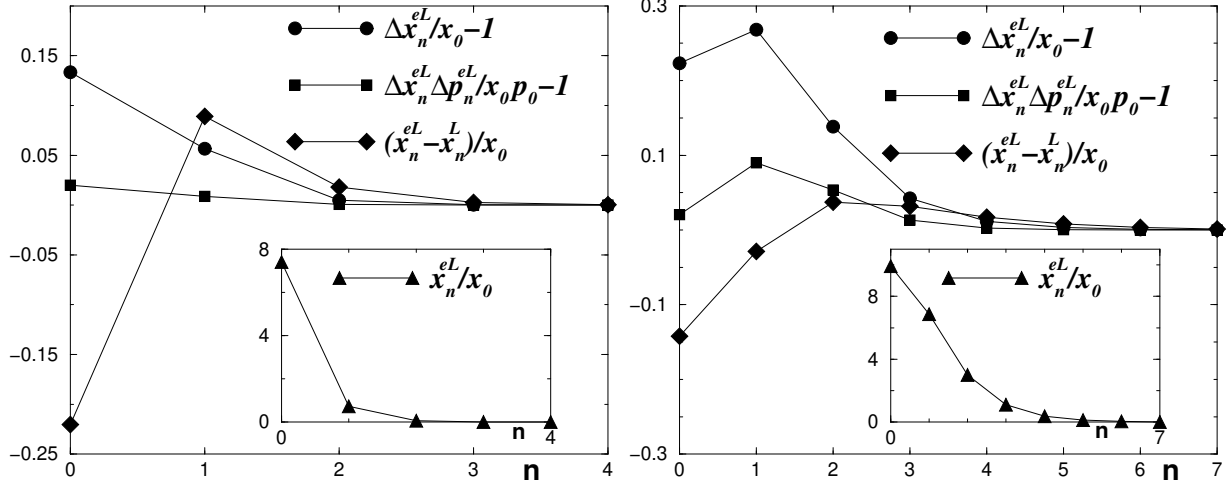


FIG. 3. Difference between the mean lattice deformation, mean uncertainty of the on-site lattice vibration and corresponding product of uncertainties for the L and eL methods. The inset shows the mean lattice deformation of the eL method. Hamiltonian parameters are $t = 10 \hbar\omega$, $g = 4.5 \hbar\omega$, and $t = 250 \hbar\omega$, $g = 16.5 \hbar\omega$, for the first and second plots, respectively.

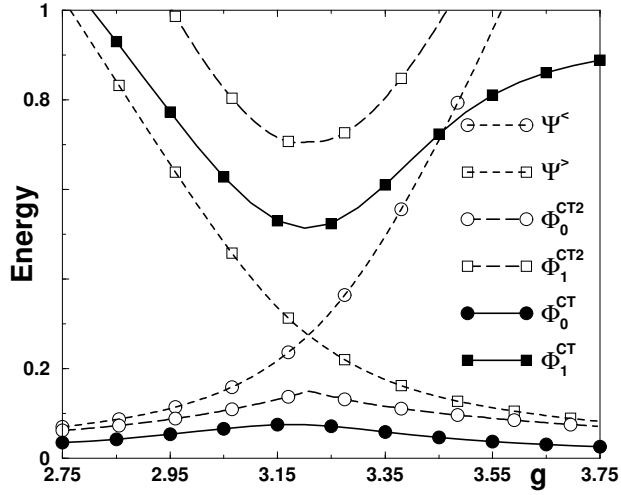


FIG. 4. The anti-crossing of $|\Psi^<>$ and $|\Psi^>>$ energies along with the ground state $|\Phi_0^{CT2}\rangle$ and first excited state $|\Phi_1^{CT2}\rangle$ energies. The results of CT method are also plotted for comparison. The ground state energy obtained by eT method is subtracted from all energy curves. $t = 5 \hbar\omega$, $K = 0$, and $\hbar\omega = 1$, while $g_{ST} = 3.24 \hbar\omega$.

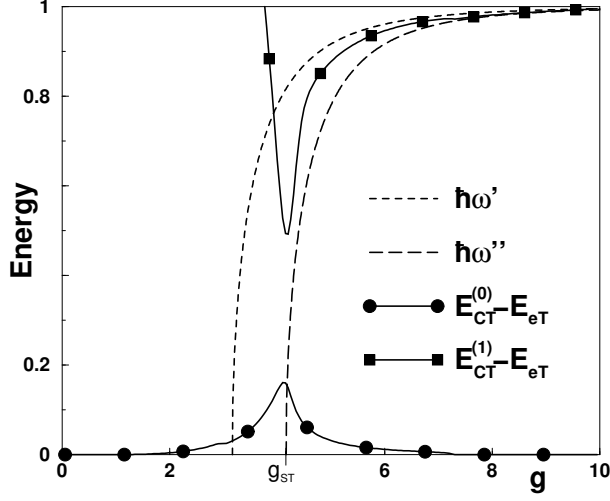


FIG. 5. The energy of the first excited state, $E_{CT}^{(1)} - E_{eT}$, computed by the CT method is compared to the energy $\hbar\omega'$ (see Eq. (24)), and $\hbar\omega''$ (see Eq. (25)). The error of the CT ground state energy, $E_{CT}^{(0)} - E_{eT}$, is shown as well. $t = 10 \hbar\omega$, $K = 0$, and $\hbar\omega = 1$, while $g_{ST} = 4.16 \hbar\omega$.

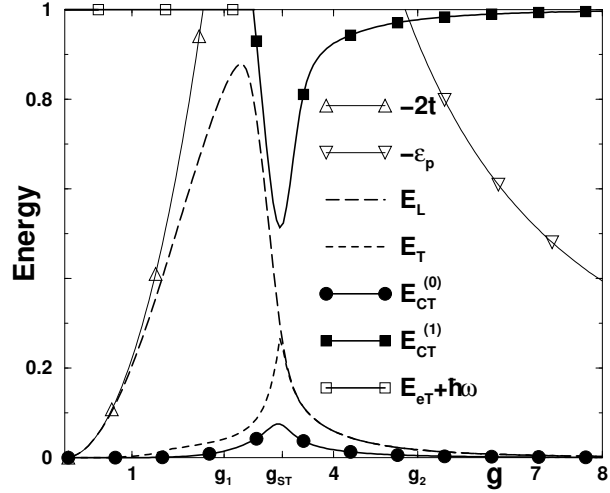


FIG. 6. The ground state energy of the polaron for various methods and the first excited state energy of the CT method are plotted for $t = 5 \hbar\omega$, $K = 0$ and $\hbar\omega = 1$. The eT ground state energy is subtracted from all results. Only the lowest $\hbar\omega$ energy interval of the spectrum, relevant for the ground and first excited energy, is shown. The $E_{eT} + \hbar\omega$ line denotes the first excited state energy, when it consists of the polaron ground state and one extra phonon, see Eq. (21).